Short Communication

Selective gas-phase catalytic fluorination of 1,1,2,3-tetrachloropropene to 2-chloro-3,3,3-trifluoropropene

CrossMark

Wei Mao, Bo Wang, Yangbo Ma, Wei Zhang, Yongmei Du, Yue Qin, Jianping Kang, Jian Lu *

Department of Catalytic Technology, Xi'an Modern Chemistry Research Institute, Xi'an 710065, Shaanxi Province, PR China
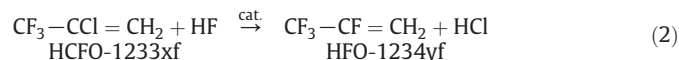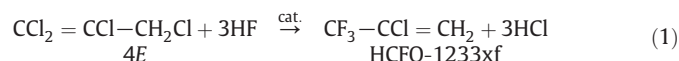
ABSTRACT

For synthesis of 2,3,3,3-tetrafluoropropene, 2-chloro-3,3,3-trifluoropropene (HCFO-1233xf) is an essential intermediate. We here report the catalytic fluorination of 1,1,2,3-tetrachloropropene (4E) to 2-chloro-3,3,3-trifluoropropene (HCFO-1233xf) over fluorinated chromia catalyst modified by Y or La. A highly selective and stable catalyst was achieved over the La promoted fluorinated chromia, where almost 100% 4E conversion and HCFO-1233xf selectivity were obtained for a 96 h TOS. The results of preliminary characterization indicated that surface CrO_xF_y species and BET area of catalyst were related with the 4E fluorination activity.

© 2014 Elsevier B.V. All rights reserved.

1. Introduction

Global warming and depletion of the atmospheric ozone have been the main environmental issues that threaten the sustainable development of the world [1]. Being the most potent and main greenhouse gases (GHG), hydrofluorocarbons (HFCs) such as 1,1,1,2,-tetrafluoroethane (HFC-134a) with a global warming potential (GWP) over 1400 are still used as refrigerants, foaming and cleaning agents [2]. Thus, more stringent legislations have been putting on the emission of potent GHGs, and this has prompted the research and development of environmentally benign alternatives to HFCs [2b,3]. Among the available choices, 2,3,3,3-tetrafluoropropene (HFO-1234yf) has been proven one of the most promising alternatives to HFCs due to its less impact on environment, i.e., GWP of 4 and zero ozone depletion [3]. Thus, the environmentally benign process for the production of HFO-1234yf becomes a recently important topic in the related domains.

$$CCl_2=CCl-CH_2Cl + 3HF \xrightarrow{cat.} CF_3-CCl=CH_2 + 3HCl \qquad (1)$$
$$\underset{4E}{} \qquad \underset{HCFO\text{-}1233xf}{}$$

$$CF_3-CCl=CH_2 + HF \xrightarrow{cat.} CF_3-CF=CH_2 + HCl \qquad (2)$$
$$\underset{HCFO\text{-}1233xf}{} \qquad \underset{HFO\text{-}1234yf}{}$$

Although there is no open report on the synthesis of HFO-1234yf, recent patents suggest a viable two-step fluorination process via the intermediate of 2-chloro-3,3,3-trifluoropropene (HCFO-1233xf) [4]. Thus the gas-phase catalytic fluorination of 1,1,2,3-tetrachloropropene (4E) to HCFO-1233xf is a crucial step for the synthesis of HFO-1234yf. In patent [4], the chromia was employed to catalyze this reaction, but fast catalyst deactivation was observed. Then, organic amine molecules like diisopropyl amine were added into the reaction material to improve the lifespan of catalyst. Possibly, these organic bases can inhibit the undesirable polymerization reaction and/or coking involving the catalyst.

Generally, the Cr-based catalysts after pretreatment with fluorine containing gases such as HF are active for the common gas-phase fluorination reactions [5]. Moreover, the catalytic fluorination of chloroethenes such as trichloroethylene has been quantitatively investigated [6], and the isolated CrF_3, $Cr(OH)_xF_y$ and CrO_xF_y (the Cr with valent $> +3$) species are suggested to be possibly active phases [7]. However, in comparison with chloroethenes, the increased carbon-chain length and the carbon–carbon double bands make the fluorination of 4E more complex. Further reaction paths are expected to decrease the selectivity of the desired product. Carbon deposition over the catalyst could be easily occurred, leading to rapid catalyst deactivation. Thus, the design of a selective and stable catalyst for the fluorination of 4E is challengeable.

Based on the coherent thoughts, the surface acidity of the Cr-based catalyst must be regulated so that the 4E fluorination could be occurred effectively and the coke deposition is greatly inhibited. More importantly, we assume that the catalytic performance is different over aforementioned active Cr species, and modifying surface

* Corresponding author. Tel./fax: +86 29 88291213.
E-mail address: lujian204@gmail.com (J. Lu).

Cr species would affect significantly the catalyst behavior in this reaction. Following these rules, La_2O_3 and Y_2O_3 were impregnated, respectively, onto the prepared chromia, which were expected to adjust the distribution of active Cr species as well as the surface acidity. The main purpose of this work is to ascertain if these modified chromia catalysts can achieve excellent performance in 4E fluorination without any organic additive. Then, for the first time, a highly active and stable La promoted chromia catalyst was developed.

2. Experimental

2.1. Preparation of catalysts

The pure chromium oxide was prepared by a precipitation method. The detailed process was as follows: a solution of aqueous ammonia (25 wt.%) was added into a stirring solution of chromium chloride at a constant rate until a pH of 7.5 was reached. Then, the precipitate obtained was filtered, washed with distilled water and dried at 120 °C for 12 h under nitrogen, followed by a calcination at 300 °C for 8 h in air. The resulting solid was powdered, mixed with 2% graphite and formed into cylindrical pellets as the blank catalyst precursor. The doped chromia catalysts were prepared by the incipient wetness impregnation method. The prepared chromia powder was impregnated by an aqueous solution of the corresponding $La(NO_3)_3$ or $Y(NO_3)_3$, subsequently dried at 120 °C overnight, and finally calcined at 300 °C for 8 h under N_2. The content of the metal salt in the solution was adjusted to giving the final metal loading of 1 wt.%.

2.2. Catalyst activation

Prior to use, the fresh oxide sample was subject to a pre-fluorination process so as to obtain an activity for the fluorination of 1,1,2,3-tetrachloropropene. The pelletized catalyst precursor (60 mL) was charged into a nickel tubular reactor with a diameter of 2.5 cm and a length of 70 cm; it was heated at 200 °C for 8 h in N_2 at a flow of 250 mL min^{-1}, then activated with a mixture stream of HF and N_2 (molar ratio of HF/N_2 = 1:4) at 250–350 °C for 12 h. The fluorinated chromia referred to F–Cr, and the fluorinated chromia promoted with La_2O_3 and Y_2O_3 was denoted as La/F–Cr and Y/F–Cr, respectively.

2.3. Catalytic fluorination

The fluorination reaction was carried out under atmospheric pressure in the same reactor at 260 °C after the preliminary fluorination of catalyst. Flow rate of HF pre-heated in a chamber at 45 °C was carefully controlled at 300 mL min^{-1} using a Sevenstar mass flowmeter, and the $CCl_2 = CCl - CH_2Cl$ feed was regulated at room temperature with a liquid pump. The molar ratio of HF/$CCl_2 = CCl - CH_2Cl$ was fixed at 10:1 and the GHSV was 300 h^{-1}. The product stream from the reactor was scrubbed with H_2O (50 °C), then passed through a drier (5 A zeolite) and finally to the GC. The organic reaction products were analyzed by a gas chromatograph (Haixin GC-930) equipped with a flame ionization detector (FID) and a DB-5 (30 m × 0.25 mm) capillary column. The relative composition of the products is based on peak areas and therefore do not represent the absolute yields because of difference in response factors. Moreover, GC–MS (Thermo Scientific ITQ 700) with a DB-5MS capillary column was used for the identity of the organic compounds formed during the reaction. The temperature for the gasification compartment was maintained at 250 °C. The temperature control program was followed by maintaining at 40 °C for 3 min and then increasing to 200 °C with an increment of 10 °C/min. The electron energy and the electron double voltage were set at 70 eV and 1200 V, respectively.

2.4. Characterization

The metal content in the sample was determined by X-ray fluorescence (XRF) spectrometer (ELEMENTAR Vario ELIII) with the uncertainty of 3%. Surface chemical compositions in the samples were analyzed using an X-ray photoelectron spectrometer (XPS) (Thermo Scientific K-Alpha) equipped with an Al monochromatic X-ray source (Al Kα = 1486.6 eV) under room temperature in high vacuum (about $1 × 10^{-9}$ Pa). Curve fitting of the narrow-scan XPS spectra was carried out with a mixed Gaussian–Lorentzian product function. Shirley background was subtracted from each spectrum before the curve fitting. The position of C1s BE at 284.8 eV was used as an internal standard for correcting any charge-induced peak shifts. Before the test, the pellet type samples were outgassed for about 2 h at 423 K under a pressure of $1 × 10^{-6}$ Pa to minimize the surface contamination. Raman spectra were obtained on a Renishaw Raman System 2000 with exciting wavelength of 785 nm under ambient conditions. XRD patterns of the prepared samples were collected with a Rigaku D/max-γA rotation anode X-ray diffractometer (Cu Kα, λ = 0.15418 nm). The surface area of the catalysts was measured using nitrogen adsorption at 77 K and the Brunauer–Emmett–Teller (BET) method using a Micromeritics ASAP2020 system. The temperature-programmed desorption of ammonia (NH_3-TPD) measurement was carried on an AutoChem II 2920 instrument (Micromeritics, USA) for comparing the acidity of various samples. Prior to TPD studies, a sample of 50 mg was first pretreated in pure He at 773 K for 60 min, then cooled to 393 K and saturated at this temperature with anhydrous ammonia gas (10% in He) for 30 min. Weakly adsorbed NH_3 was eliminated by treatment under He at the same temperature for 60 min. The NH_3-TPD profile was recorded with a thermal conductivity detector with a heating rate of 10 K min^{-1} from 393 to 673 K in a He flow.

3. Results and discussion

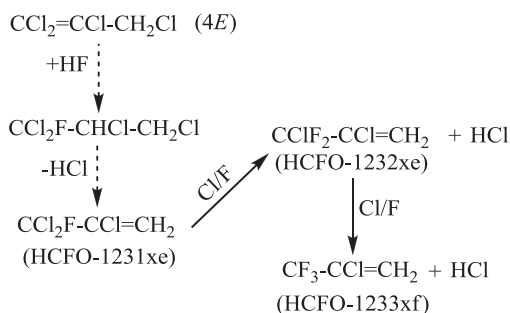### 3.1. Fluorination of 4E over Cr-based catalysts

Fig. 1 displays the time-on-stream (TOS) results of 4E fluorination. Each catalyst showed high initial activity (100% conv. for 4E) and selectivity to HCFO-1233xf (>98%). However, only the La/F–Cr catalyst sustained almost full 4E conversion and HCFO-1233xf selectivity over a 96 h TOS. Conversely, above indexes decreased gradually with time over the F–Cr catalyst, which were reduced by 12.4% and 12.1%, respectively, after 96 h. The Y/F–Cr catalyst exhibited the poorest stability in comparison with other catalysts, where the 4E conversion and HCFO-1233xf selectivity were reduced by 26% and 32.2%, respectively, after reaction. These results clearly indicate that the dopant La has positive promotional effect on the property of fluorinated chromia, whereas the addition of Y exhibits negative promotional effect. Thus, La_2O_3 is required to improve catalytic behavior of fluorinated chromia for the production of HCFO-1233xf.

On the other hand, introducing La or Y into chromia exhibited little effect on the initial product distribution. Besides HCFO-1233xf, the other minor components formed were 2,3-dichloro-3,3-difluoropropene (HCFO-1232xe), 1,2-dichloro-3,3,3-trifluoropropene (HCFO-1223xd), and 2,2,3-trichloro-1,1,1-trifluoropropane (HCFC-233ab) with trace amounts of 2,3,3-trichloro-3-fluoropropene (HCFO-1231xe), 2-chloro-1,1,1,2-tetrafluoropropane (HCFC-244bb), 2,3-dichloro-1,1,1-trifluoropropane (HCFC-243db) and HFO-1234yf in all the experiments. The total selectivity to byproducts was less than 2% at the initial stage of reaction. However, it is worth noting that the content of less fluorinated compounds HCFO-1232xe and HCFO-1231xe increased gradually over time on the F–Cr and Y/F–Cr. Especially the HCFO-1232xe selectivity, it reached to 10% and 28%, respectively after 96 h TOS over the F–Cr and Y/F–Cr catalysts. At the same time, the HCFO-1231xe selectivity reached to 2% and 3%, respectively. Regardless of catalyst, the selectivity to other fluorinated
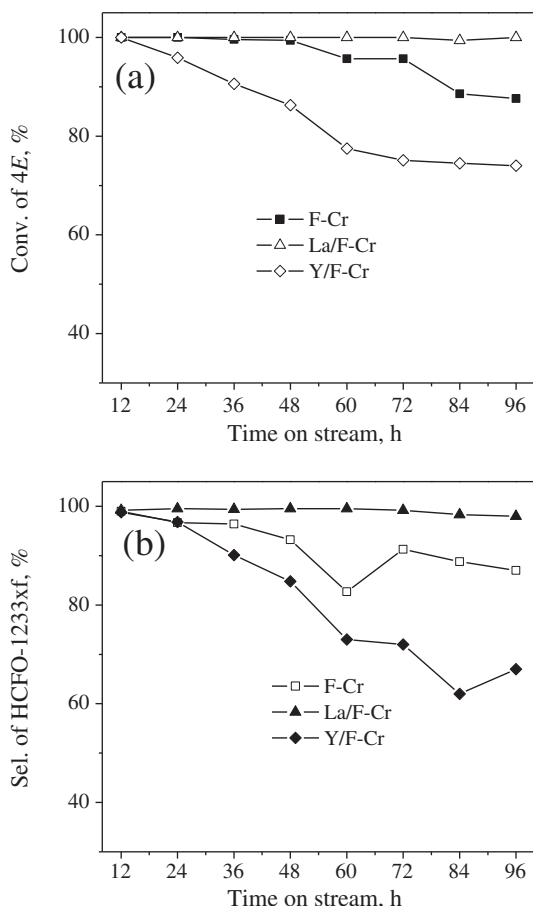
Fig. 1. Catalytic performances of various fluorinated Cr-based catalysts for 4E fluorination with HF. (a) conversion of 4E vs. time on stream; (b) selectivity of HCFO-1233xf vs. time on stream.

byproducts did not change significantly. Obviously, the greater catalyst deactivation, the larger content of HCFO-1232xe and HCFO-1231xe. Based on the information of product distribution, it is rational to presume that HCFO-1232xe and HCFO-1231xe are the main intermediates during 4E fluorination. While we find it difficult to clarify every intermediate in 4E fluorination at the moment, some speculation on the reaction pathway can be obtained according to general recognition for heterogeneous fluorination of chloroalkenes [7a,8]. Scheme 1 displays a simplified reaction pathway for fluorination of 4E to HCFO-1233xf. In general, a C—Cl bond at a double bonded carbon is significantly stronger than that of a single bonded C-atom, indicating that direct Cl/F exchange is difficult at the unsaturated C-atoms.

Hence, the transformation of 4E to HCFO-1231xe may run via the consecutive HF-addition followed by HCl elimination processes, although the intermediate 1,1,2,3-tetrachloro-1-fluoropropane was not detected. However, observing the molecular structure, the group CCl_2F- of HCFO-1231xe can be hardly fluorinated to $CClF_2-$ via the addition/elimination process. The direct Cl against F exchange is more possible in the fluorination of HCFO-1231xe to HCFO-1232xe. Similar process may also occur in the fluorination of HCFO-1232xe to HCFO-1233xf.

3.2. Characterization of catalysts

To find out the reasons that affected the catalysts' behaviors, different Cr-based catalysts were characterized by XRD. As shown in Fig. 2, all the samples exhibited only a broad diffuse peak with high background intensities, indicating that typical amorphous structure or microcrystalline phase was predominant in each fluorinated catalyst. Indeed, the Cr species formed after treatment with HF were highly dispersed on the surface of catalyst in all the samples. The detailed molecular structure of the Cr species was further probed by the Raman spectroscopy (Fig. 3). For chromia, only a broad peak at 835 cm^{-1} was observed, which can be assigned to symmetrical stretching of monomeric chromate species (Cr^{6+}) [7b]. This result indicates that the chromium with oxidation state VI was present in the prepared chromia, the molar ratio of Cr^{3+}/Cr^{6+} was estimated to 3.2 according to the XPS analysis. Previous studies have reported similar formation of oxidized Cr-species (Cr > 3+) on the surface of chromia [7c–e]. After fluorination, above characteristic Raman band was also observed for the F—Cr sample but clearly shifted (near 869 cm^{-1}). Furthermore, two new bands at 1319 and 1581 cm^{-1} appeared in the spectra of the F—Cr sample, which can be assigned to stretching of the $Cr^{VI}O_xF_y$ species formed during the activation [7b]. The La/F—Cr sample showed the same Raman bands of chromate and CrO_xF_y species as the F—Cr sample. In contrast, only a Raman band of chromate species was observed for the Y/F—Cr sample and the band of the CrO_xF_y species was not detected. On the other hand, the peak intensity of chromate species was weakened significantly for the fluorinated samples except the Y/F—Cr. These Raman spectra results indicate that isolated chromate species were transformed into CrO_xF_y species during the pre-fluorination for the F—Cr and La/F—Cr samples, while for the Y/F—Cr sample this process was not taken place.

To reveal the upmost surface species, XPS was applied for different fluorinated catalysts, and the results are given in Fig. 4. For the F—Cr and La/F—Cr samples, the deconvolution of Cr2$p_{3/2}$ gives three species of Cr(OH)$_3$ [Cr(I)], CrF$_3$ [Cr(II)] and CrO$_x$F$_y$ [Cr(III)] with the BE values of 579, 581.8 and 584.6 eV, respectively [9]. Conversely, apart from the Cr(OH)$_3$ and CrF$_3$ species, the deconvolution of Cr2$p_{3/2}$ for the Y/F—Cr sample gives a different species of Cr(OH)$_x$F$_y$ with BE value of 583.4 eV [7d]. The XPS results confirm that different chromium species

Scheme 1. Possible reaction paths for the fluorination of 4E catalyzed by Cr-based catalysts.
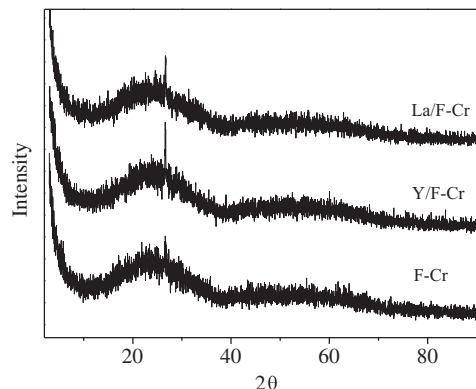
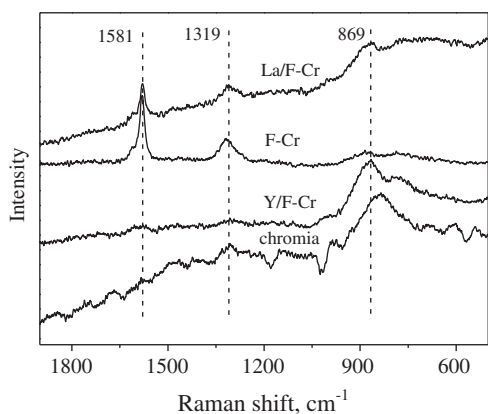**Fig. 2.** X-ray diffractograms for various fluorinated Cr-based catalysts.

Fig. 3. The Raman spectra of various fluorinated Cr-based catalysts.

were present on the fluorinated catalysts. The CrO_xF_y species were only formed for the F–Cr and La/F–Cr samples. This is consistent with the results of Raman spectra. Furthermore, the atom ratio of surface Cr(II)/Cr(III) decreases from 3.9 to 3.5 after introducing La onto chromia, indicating that more CrO_xF_y species were formed during the activation for the La/F–Cr. The NH$_3$-TPD is used for investigating the strength of

acid sites present on the surface of various catalysts. It can be observed from Fig. 5 that a broad desorption profile in the range 120–400 °C appears in all the samples with one maximum peak around 200 °C. This suggests that weak acid sites are predominant on the surface of prepared Cr-based catalysts.

As mentioned above, catalytic activity over Cr-based catalyst is related to the presence of chromium fluorides or oxyfluoride species after the activation by HF. The XRD, Raman spectra and XPS results reveal that both F–Cr and La/F–Cr catalysts contained isolated CrO_xF_y and CrF_3 species, while the Y/F–Cr catalyst contained isolated $Cr(OH)_xF_y$ and CrF_3 species. Moreover, the quantitative XPS results show that a higher CrO_xF_y content was obtained in the La/F–Cr than in the F–Cr. Trunschke et al. have revealed that the addition of La can improve the dispersion of surface chromium oxide species [10], while the monomeric chromate species are easier fluorinated than the oligomeric chromate species [7b]. Thus, our results suggested that the addition of La could also favor the formation of active specie CrO_xF_y during the activation. Luo et al. have reported that the $Cr(OH)_xF_y$ species can be formed in the Cr–Y catalyst [7d]. Our results are in good agreement with theirs. Therefore, the role of different dopants can be ascribed to adjusting the distribution of active Cr species on the catalyst. The difference of surface CrO_xF_y content coincided exactly with the catalytic behaviors of various catalysts, where the most active and stable catalyst for 4E fluorination was the La/F–Cr with maximum CrO_xF_y species. Therefore, it
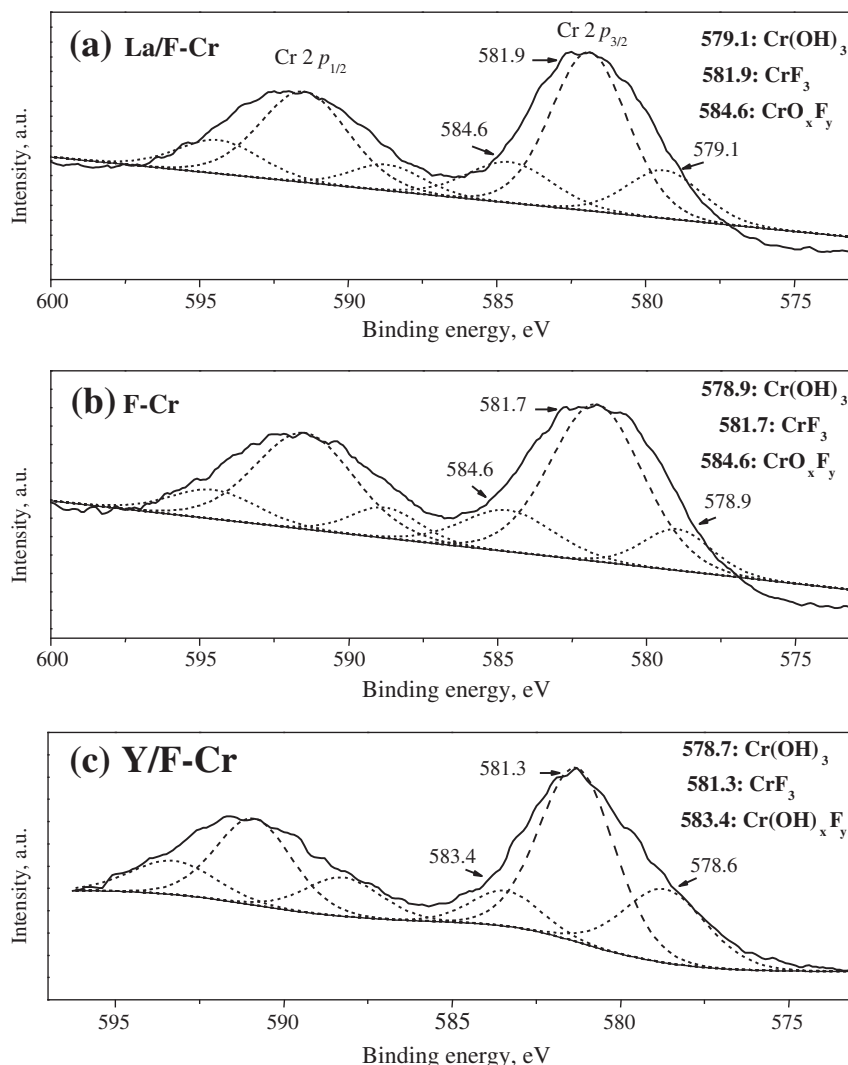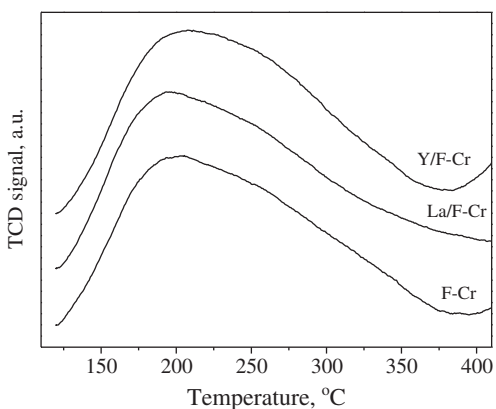

Fig. 4. The XPS spectra of Cr2p for various fluorinated Cr-based catalysts.

Fig. 5. The profiles for temperature-programmed desorption of ammonia on various fluorinated Cr-based catalysts.

can be concluded that dispersed CrO_xF_y species are mainly responsible for the fluorination of 4E to HCFO-1233xf. In addition, for gas-phase fluorination, high surface area catalyst is crucial to achieve high activity and long lifetime [6c]. Nevertheless the fluorination of metal oxides leads generally to an important decline of the surface area. Following the aborative pre-fluorination, the fluorinated chromia with high surface area was obtained in this work, 96 m^2 g^{-1} to F–Cr, 105.5 m^2 g^{-1} to Y/F–Cr and 114.2 m^2 g^{-1} to La/F–Cr, respectively. These values are comparable to that reported for porous fluorinated chromia (105.1 m^2 g^{-1}) [11]. Thus, the high activity and stability of La/F–Cr can be also ascribed to its large surface area.

Since the 4E conversion still achieved more than 70% after 96 h TOS in all catalysts, this indicates that other active Cr species like CrF_3 and $Cr(OH)_xF_y$ were also responsible for catalyst activity. But the HCFO-1233xf selectivity declined remarkably over the F–Cr and Y/F–Cr, indicating that 4E cannot be entirely fluorinated on above active centers. It is well-known that the coke formation primarily accounts for the catalyst deactivation in the fluorination catalysis [6c,9a]. Based on the XPS analysis, the surface C content was increased by 49%, 62% and 73% for La/F–Cr, F–Cr and Y/F–Cr, respectively, after 4E fluorination. Thus, it is reasonable to infer that the catalyst deactivation is related with carbon deposition in this reaction. The HCFO-1233xf selectivity and 4E conversion could decrease gradually as the active Cr species like CrO_xF_y were reduced by carbon deposition. The differences of active species and BET surface make different activities and stabilities for various Cr-based catalysts. The poor performance of Y/F–Cr can be due to the absence of active specie CrO_xF_y.

4. Conclusion

In summary, gas-phase fluorination of 4E to HCFO-1233xf can be performed on the fluorinated chromia using La as a promoter with a highly catalytic activity and long lifetime, and a reasonable reaction pathway was proposed. The characterization results revealed that excellent catalytic performance was relevant to the CrO_xF_y species and large surface area of Cr-based catalyst. The addition of La can improve the content of CrO_xF_y species on the fluorinated chromia. We anticipate our discovery to be a starting point for developing effective chromia-based catalysts for synthesis of the hydrofluoroolefin by heterogeneous fluorination and will promote the commercialization of HFO-1234yf.

References

[1] J.M. Last, Annu. Rev. Public Health 14 (1993) 115–136.
[2] (a) K.P. Shine, W.T. Sturges, Science 315 (2007) 1804–1805;
    (b) G.J.M. Velders, A.R. Ravishankara, M.K. Miller, M.J. Molina, J. Alcamo, J.S. Daniel, D.W. Fahey, S.A. Montzka, S. Reimann, Science 335 (2012) 922–923.
[3] (a) S. Papasavva, D.J. Luecken, R.L Waterland, K.N. Taddonio, S.O. Andersen, Environ. Sci. Technol. 43 (2009) 9252–9259;
    (b) S. Papasavva, D.J. Luecken, R.L Waterland, K.N. Taddonio, S.O. Andersen, Environ. Sci. Technol. 44 (2010) 343–348.
[4] (a) M.Y. Elsheikh, P. Bonnet, B.B Chen, US Patent 8076521 (2011)
    (b) D. Deur-bert, L. Wendlinger, A. Pigamo, US Patent 8207383 (2012)
    (c) D.C. Merkel, H.S. Tung, US Patent 8119845 (2012).
[5] (a) J. Barrault, S. Brunet, B. Requieme, M. Blanchard, Chem. Commun. (1993) 374–375;
    (b) D.W. Bonniface, J.R. Fryer, P. Landon, J.D. Scott, W.D.S. Scott, M.J. Watson, G. Webb, J.M. Winfield, Green Chem. (1999) 9–11;
    (c) B. Adamczyk, O. Boese, N. Weiher, S.L.M. Schroeder, E. Kemnitz, J. Fluorine Chem. 101 (2000) 239–246.
[6] (a) L.E. Manzer, Science 249 (1990) 31–35;
    (b) L.E. Manzer, V.N.M. RAO, Adv. Catal. 39 (1993) 329–350;
    (c) L.E. Manzer, M.J. Nappa, Appl. Catal. A 221 (2001) 267–274.
[7] (a) A. Kohne, E. Kemnitz, J. Fluorine Chem. 75 (1995) 103–110;
    (b) D.H. Cho, Y.G. Kim, M.J. Chung, J.S. Chung, Appl. Catal. B 18 (1998) 251–261;
    (c) J.M. Rao, A. Sivaprasad, P.S. Rao, B. Narsaiah, S.N. Reddy, V. Vijayakumar, S.V. Manorama, K.L. Krishna, K. Srinivas, K.R. Krishnan, S. Badrinarayanan, J. Catal. 184 (1999) 105–111;
    (d) J. He, G.Q. Xie, J.Q. Lu, L. Qian, X.L. Zhang, P. Fang, Z.Y. Pu, M.F. Luo, J. Catal. 253 (2008) 1–10;
    (e) S. Brunet, B. Requieme, E. Colnay, J. Barrault, M. Blanchard, Appl. Catal. B 5 (1995) 305–317.
[8] M. Bankhead, G.W. Watson, G.J. Hutchings, J. Scott, D.J. Willock, Appl. Catal. A 200 (2000) 263–274.
[9] (a) H. Lee, H.D. Jeong, Y.S. Chung, H.G. Lee, M.J. Chung, S. Kim, H.S. Kim, J. Catal. 169 (1997) 307–316;
    (b) Y.S. Chung, H.J. Lee, H.D. Jeong, Y.K. Kim, H.G. Lee, H.S. Kim, S. Kim, J. Catal. 175 (1998) 220–225.
[10] A. Trunschke, D.L. Hoang, J. Radnik, H. Lieske, J. Catal. 191 (2000) 456–466.
[11] X.Q. Jia, H.D. Quan, M. Tamura, A. Sekiya, RSC Adv. 2 (2012) 6695–6700.